*URSI AP-RASC 2019, New Delhi, India, 09 - 15 March 2019*

# Stub loaded hexagonal open loop band pass filter with improved selectivity

Harikrishnan A I[(1)], S. Mridula[(1)],P. Mohanan[(2)],
(1) Division of Electronics Engineering,
School of Engineering,
Cochin University of Science and Technology,
Kochi 682022, India.
(2) Department of Electronics, Cochin University of Science and Technology,
Kochi 682022, India.

## Abstract

A stub loaded hexagonal open loop band pass filter is presented in this paper. The filter operates in the 850 MHz - 950 MHz band and shows good skirt selectivity. A detailed theoretical analysis of the even and odd modes of excitation of the resonator is performed. The prototype of the filter is fabricated on substrate C-MET LK4.3 with dielectric constant 4.3 and loss tangent 0.0018. The measured results exhibit good agreement with the simulation. The electrical size of the resonator is 0.18 $\lambda_g$ x 0.303 $\lambda_g$; when $\lambda_g$ = 187.5 mm.

## 1. Introduction

Planar microstrip Band Pass Filters (BPF) are indispensable in the RF front ends of both the receiver and transmitter in modern wireless communication systems. Conventionally, single or dual mode resonators are used to design microstrip band pass filters. Dual mode resonator filters are advantageous over single mode resonator filters because they behave as doubly tuned circuits, making use of both odd and even mode resonances. This helps to reduce the number of resonators required for designing filter of given order [1]-[2].

Different types of dual-mode microstrip BPF using patch resonators and loop resonators are reported in [3]-[12]. Loop resonators are either closed loop or open loop. A dual mode dual band BPF is proposed in [5]. In [6] a stepped impedance stub loaded square open loop resonator filter is presented. A stub loaded BPF with four transmission zeroes on either side of both pass bands is reported in [7] and a wide BPF using signal interference principle is presented in [8]. A dual mode open loop resonator with two additional transmission zeros for improving stop-band performance is presented in [9] and a technique to improve selectivity using lumped and quasi lumped elements is proposed in [10].A pair of coupled U-shaped resonators behaving as a dual-band resonator is reported in [11]. A narrow BPF with two resonators is reported in [12]. In all the above reported designs, it is observed that skirt selectivity is only in one of the two sides of pass band and also number of resonators has to be increased to improve the selectivity. This paper presents a triple mode BPF with high skirt selectivity on either side of the pass band.

## 2. Filter Structure

Fig.1(a) shows the layout of the proposed filter. The triple mode filter is developed from a dual mode resonator consisting of a stepped impedance stub ($S_1$) of dimensions $L_{11}$, $W_{11}$, $L_{12}$, $W_{12}$ loaded into a Hexagonal Open Loop Resonator(HOLR) of dimensions $L_{01}$, $L_{02}$, $L_{03}$, $W_{01}$. An additional stepped impedance stub ($S_2$) of dimensions $L_{22}$, $W_{11}$, $L_{21}$, and $W_{21}$ is connected to the dual mode resonator to introduce a third resonance. The resonator is excited using a 50Ω micro strip transmission line of dimension $L_{txn}$, $W_{txn}$. The coupling at the two ports is enhanced using sections of hexagonal stubs of dimension $CL_1$, $CL_2$, $CL_3$, CW. The bottom plane acts as ground. The filter is designed on substrate CMET LK 4.3 with dielectric constant 4.3, height 1.6 mm and loss tangent 0.0018. The overall size of the filter is 0.27 $\lambda_g$ x 0.43 $\lambda_g$. The simulated transmission and reflection characteristics are shown in Fig 1(b). CST Microwave studio is used for simulation studies.

The filter exhibits two even mode resonances $f_{el}$ (0.86GHz), $f_{eu}$(0.95 GHz) and one odd mode resonance $f_o$(0.9GHz). The even and odd mode analysis of the resonator is detailed in Section 3. The lower edge of the pass band is determined by the lower even mode frequency $f_{el}$, which is due to HOLR and stepped impedance stub $S_2$. The upper edge of the pass band is determined by the upper even mode frequency $f_{eu}$ , which is due to HOLR and stepped impedance stub $S_1$.The hexagonal loop is half wavelength long at the frequency $f_o$. Generally for dual mode resonators, the transmission zero is on the higher side of the two modes when the even mode is higher than the odd mode frequency. On the other hand transmission zero will be on the lower side of the two modes when even mode frequency is less than the odd mode frequency. This property is used to design the band pass filter [1].

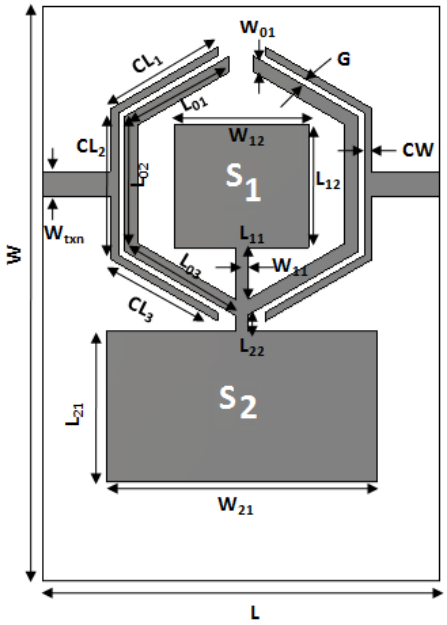


Fig.1(a) Layout of the proposed filter $CL_1$ = 15.5, $CL_2$ = 17.9, $CL_3$ = 15.5, CW = 1.1, $L_{01}$ = 15.2, $L_{02}$ = 16, $L_{03}$ = 16, $W_{01}$ = 2, $L_{12}$ = 15.5, $W_{12}$ = 17, $L_{11}$ = 6.5, $W_{11}$ = 1.5, $L_{21}$ = 19, $W_{21}$ = 34, $L_{22}$ = 1.9, G = 0.4, W = 80, L= 50, $L_{txn}$= 9, $W_{txn}$= 3 (All dimensions in mm) Substrate : $\varepsilon_r$= 4.3, height = 1.6mm, loss tangent = 0.0018.

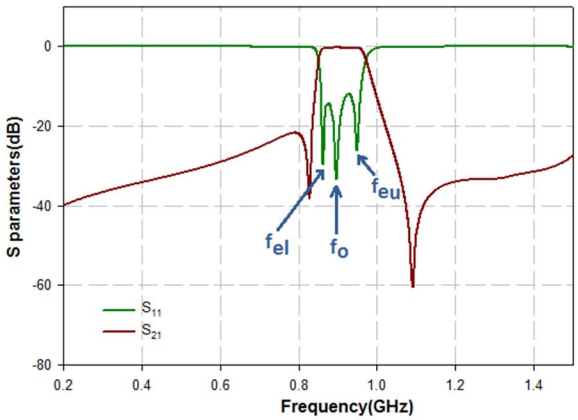


Fig. 1(b) Simulated transmission and reflection characteristics of the proposed filter

## 3 Theoretical analysis of the stub loaded hexagonal open loop resonator

Fig.2 shows the structure of the stub loaded hexagonal open loop resonator. Since the structure is symmetric, even-odd mode analysis can be used to analyze the resonator. The resonator under even and odd mode excitation is shown in Fig. 3a, Fig. 3b and Fig.3c.

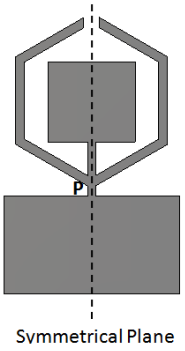


Fig.2 Stub loaded Hexagonal Open Loop Resonator

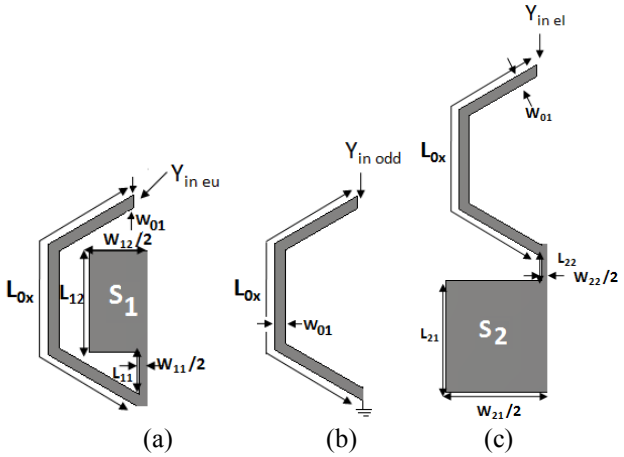


Fig. 3 Equivalent structure of resonator under (a) upper even mode resonance (b) odd mode resonance (c) lower even mode resonance

### 3.1 Odd mode Analysis

In odd mode excitation, voltage null exist at the midpoint (P) of the hexagonal open loop Fig.2. At 0.9 GHz the current is crowded only in the hexagonal loop thus identifying it as the contributing element for the odd mode as illustrated in Fig.4.

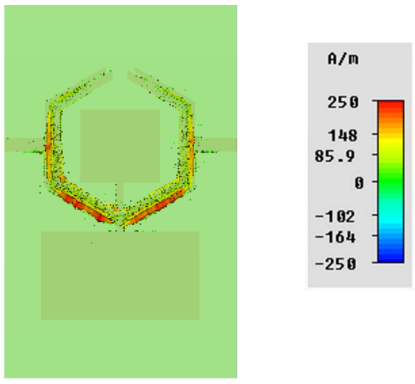


Fig.4 Surface current distribution at 0.9 GHz

Exploiting the symmetry, at the odd mode can be equivalently represented as shown in Fig.3b. The input impedance [7] for odd mode can be expressed as

$$Z_{in\,odd} = j\frac{tan\,\theta_{0o}/_2}{Z_0}$$

where $\theta_{0o}$ is the electrical length at frequency $f_o$, corresponding to the physical length $L_{0x}$. $Z_0$ is the characteristic impedance of transmission line with width $W_{01}$. At resonance $Y_{inodd} = 0$, the odd mode resonant frequency can be expressed as

$$f_o = \frac{c}{\lambda_{go}\sqrt{\varepsilon_{eff1}}}$$

Where $L_{0x} = \frac{\lambda_{go}}{4}$; $L_{0x} = L_{01} + L_{02} + L_{03}$ [Fig.1].

Effective dielectric constant $\varepsilon_{eff1}$ corresponds to the width $W_{01}$. The odd mode frequency is not affected by stepped impedance stubs loaded into the HOLR.

## 3.2 Even mode analysis

A similar study of surface current distribution is conducted at even mode frequencies $f_{el}$ (0.86 GHz) and $f_{eu}$ (0.95 GHz). At 0.86 GHz current is crowded in the hexagonal loop and the lower stub $S_2$ and at 0.95 GHz current crowding takes place in the hexagonal loop and upper stub $S_1$ thus identifying these as the contributing elements for the even modes as illustrated in Fig.5

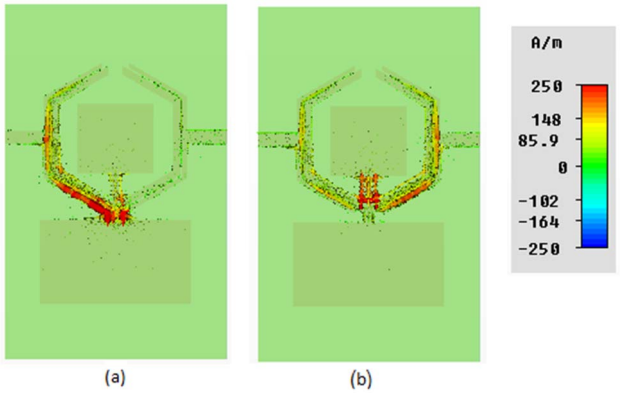


Fig.5 Surface current distribution at (a) 0.86 GHz (b) 0.95 GHz

Since there is no current flow through symmetrical plane in even mode excitation, the structure can be bisected through the symmetrical plane with open circuit at the middle to obtain the equivalent structure as shown in Fig.3a and Fig 3c. $\theta_{12eu}, \theta_{11eu}$ and $\theta_{0eu}$ are electrical lengths at frequency $f_{eu}$ corresponding to physical length $L_{12}$, $L_{11}$ and $L_{0X}$. $Z_{12}, Z_{11}$ and $Z_0$ correspond to characteristic impedance of the transmission line section with width $\frac{W_{12}}{2}, \frac{W_{11}}{2}$ and $W_{01}$ respectively. The input impedance $Z_{ineu}$ of the structure is

$$Z_{ineu} = Z_0\left[\frac{Z_{11}\frac{(R_{Z1}-tan\theta_{11eu}tan\theta_{12eu})}{j(tan\theta_{12eu}+R_Ztan\theta_{11eu})} + jZ_0tan\theta_{0eu}}{Z_0 + \frac{jZ_1(R_{Z1}-tan\theta_{11eu}tan\theta_{12eu})tan\theta_{0eu}}{j(tan\theta_{12eu}+R_{Z1}tan\theta_{11eu})}}\right]$$

Where $R_{Z1} = \frac{Z_{12}}{Z_{11}}$

$$tan\theta_{11eu} = \left[\frac{(Z_0tan\theta_{12eu} + Z_{11}R_{Z1}tan\theta_{0eu})}{(Z_{11}tan\theta_{0eu}tan\theta_{12eu} - Z_0R_{Z1})}\right]$$

The theoretical approach is validated through simulations using AppCAD. The simulated and theoretical length of different sections of resonator [Fig.3 (a)] at frequencies 0.97GHz ($\varepsilon_r$=4.3, h=1.6mm) and 1 GHz ($\varepsilon_r$= 3.5, h=0.8mm) frequency are listed in Table.1.

| $\varepsilon_r$=4.3,h=1.6mm,f=0.97GHz | | | | $\varepsilon_r$=3.5,h=0.8mm,f=1GHz | | | |
|---|---|---|---|---|---|---|---|
| Electrical Length | Simulated (radian) | Theoretical (radian) | % error | Electrical Length | Simulated (radian) | Theoretical (radian) | % error |
| $\theta_o$ | 1.75 | 1.746 | 0.23 | $\theta_o$ | 1.7 | 1.702 | 0.12 |
| $\theta_{11}$ | 0.23 | 0.234 | 1.74 | $\theta_{11}$ | 0.22 | 0.223 | 1.36 |
| $\theta_{12}$ | 0.6 | 0.597 | 0.5 | $\theta_{12}$ | 0.58 | 0.579 | 0.17 |

Table.1 Simulated and theoretical length of different sections of resonator

## 5. Experimental results

Fig.6 shows the photograph of the fabricated filter. Measurements are conducted using PNA E8362B Vector network analyser. The measured and simulated characteristics of the proposed filter are shown in Fig.7 (a-b). The filter exhibits a Fractional Bandwidth of 12.2 % with centre frequency 0.9 GHz. The measured average insertion loss is 1.6 dB in the pass band, including the connector loss. The measured attenuation is less than 20 dB in the lower stop band and 35 dB in upper stop band. The filter has two transmission zeroes located at 0.812 GHz and 1.1 GHz with attenuation 34.3 dB and 69 dB respectively. The simulated and measured results are in good agreement.

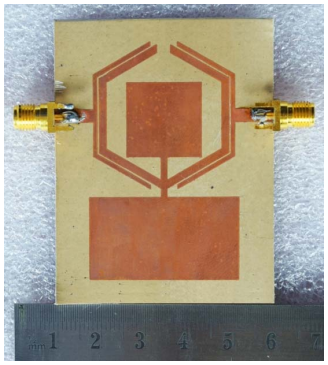

Fig.6 Photograph of the fabricated band pass filter.

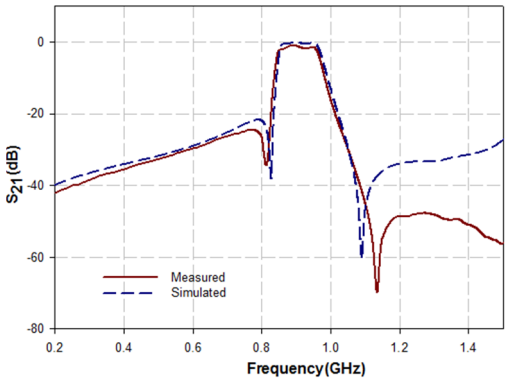


(a)

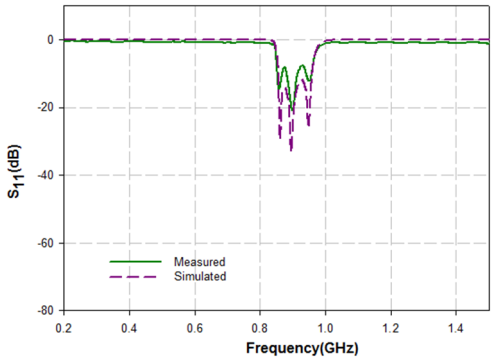

(b)

Fig.7 Measured and simulated characteristics of the proposed filter (a) $S_{21}$ (b) $S_{11}$

## 6. Conclusion

A stub loaded hexagonal open loop resonator band pass filter is presented in this paper. The filter operates in ISM band (850MHz - 950MHz). The resonator structure supports three resonant modes in the pass band and they are not mutually coupled. The symmetric nature of the resonator helps in even odd mode analysis and to deduce a relation among electrical lengths of various sections of resonators. The measured results agree well with simulated results.

## 7. References


1. Hong., Jia-Shen G., and Michael J. Lancaster, "Microstrip filters for RF/microwave applications," *John Wiley & Sons,*2004, doi:10.1002/0471221619

2. Huang, X. D., and C. H. Cheng, "A novel coplanar-waveguide bandpass filter using a dual-modesquare-ring resonator," *IEEE microwave and wireless components letters*,**16**,January 2006, pp.13–15,doi:10.1109/LMWC.2005.861358

3. Hong., Jia-Sheng., Hussein Shaman., and Young-Hoon Chun, "Dual-mode microstrip open-loop resonators and filters," *IEEE Transactions on Microwave Theory and Techniques*,**55**, August 2007, pp.1764–1770, doi:10.1109/TMTT.2007.901592

4. Serrano, Ariana Lacorte Caniato, "Synthesis methodology applied to a tunable patch filter with independent frequency and bandwidth control,"*IEEE Transactions on Microwave Theory and Techniques*, **60**, March 2012,pp. 484–493, doi: 10.1109/TMTT.2011.2181533

5. Kuo J T, Lu Y T, Lin H M, "Planar dual-mode dual-band dual-ring resonator bandpass filter*", "IEEE MTT-S International Conference on Numerical Electromagnetic and Multiphysics Modeling and Optimization for RF, Microwave, and Terahertz Applications (NEMO)*, May 2017, pp. 4-6, doi: 10.1109/NEMO.2017.7964168

6. Hong., Jia-Sheng., Hussein Shaman, and Young-Hoon Chun, "Dual-mode microstrip open-loop resonators and filters", *IEEE Transactions on Microwave Theory and Techniques,* **55,** August 2007, pp.1764–1770, doi:10.1109/TMTT.2007.901592

7. Xiu Yin Zhang, Jian-Xin Chen, QuanXue; Si-Min Li, "Dual-band bandpass filter using stub-loaded resonator", *IEEE Microwave and Wireless Components Letters*,**17**, August 2007, pp. 583–585, doi:10.1109/LMWC.2007.901768.

8. Sánchez-Soriano, Miguel Á., and Roberto Gómez-García. "Sharp-rejection wide-band dual-band bandpass planar filters with broadly-separated passbands" , *IEEE Microwave and Wireless Components Letters*, **25**, 2015,pp. 97-99,doi: 10.1109/LMWC.2014.2382669

9. Athukorala, Lakshman, DjuradjBudimir, and Milka M. Potrebic, "Design of open-loop dual-mode microstrip filters," *Progress In Electromagnetics Research Letters* , **19**,2010, pp. 179–185,doi: 10.2528/PIERL10102007.

10. Marín, Sandra, Jorge D. Martínez, and Vicente E. Boria. "Realization of filters with improved selectivity using lumped and quasi-lumped terminating half sections." *IEEE European Microwave Conference (EuMC),* 2017, pp. 636-639, doi : 10.23919/EuMC.2017.8230928

11. Ogbodo, E., Yi Wang, and Kenneth S K Yeo, "Microstrip dual-band bandpass filter using U-shaped resonators", Progress In Electromagnetics Research Letters, **59,** January 2016,pp. 1–6,doi: 10.2528/PIERL15072303.

12. Chen, S., Shi, L.Fand Xun, J.H., "An alternate circuit for narrow-bandpass elliptic microstrip filter design", *IEEE Microwave and Wireless Comp Letters*, **27**, July 2017, pp.624-626, doi:10.1109/LMWC.2017.2711528